This is the author's final version of the contribution published as:

The publisher's version is available at:

Inverse modelling of snow depths

Uwe Schlink[1], Daniel Hertel

Dept. Urban and Environmental Sociology, Helmholtz Centre for Environmental Research – UFZ, Permoserstr. 15, D-04318 Leipzig, Germany

Abstract

For inclusion into operational snow forecasting we suggest a Bayesian procedure estimating from past observations site-specific parameters with confidence intervals, based on a snow surface model, and extended by a parameterization scheme for the often not routinely registered incoming long-wave radiation. This inverse model is validated with simulated data. Simultaneous estimation of all parameters proved to be less biased. Performance is assessed for data gathered at three meteorological stations during a 2.5-year-period and also for a period of 51 years.

We found that snow albedo was 0.94, 0.89, and 0.56, snow emissivity was 0.88, 0.92, and 0.99, and snow density (in g/cm^3) was 0.14, 0.05, and 0.11 for the stations Wasserkuppe, Erfurt-Weimar, and Artern, respectively. The soil heat flux estimation was very poor; quality of snow density estimates was best. The inverse approach is recommended for snow forecasts at sub-alpine stations with more or less urban impact.

Key words: Bayesian estimation; operational snow forecasting; prediction performance; sub-alpine snow cover

[1] Corresponing author; Email: uwe.schlink@ufz.de; Tel.: +49 341 235 1554; Fax: +49 341 235 45 1554

1 Introduction

A physically based point snow surface model (Energy balance Snow Cover Integrated Model - ESCIMO) has been developed (Strasser et al., 2002) and implemented in a spreadsheet (ESCIMO.spread; (Strasser and Marke, 2010)) as an easy-to-use and portable software tool for the hourly simulation of the energy balance, the water equivalent and melt rates of a snow cover. This one-dimensional approach assumes the snow cover to be a single and homogeneous pack and solves the energy and mass balance equations for the snow surface assuming simple parameterizations of the relevant processes.

ESCIMO simulations require the specification of parameters. While some of them are physical constants (such as the specific heat of snow or the melting heat of ice), others strongly refer to the situation that is under consideration. The latter comprise (Strasser and Marke, 2010) the soil heat flux, snow albedo, emissivity of snow, clear sky emissivity, density of snow, a recession factor characterizing the albedo changes during ageing of snow, the threshold snowfall needed for the albedo to switch from old (aged) to new snow, a temperature threshold for the detection of the precipitation phase (liquid or solid), and two parameters relating the sensible and the latent heat flux to wind speed (Kuchment and Gelfan, 1996).

Many of the model parameters can be derived from site measurements or from remote sensing data, applying the AMUNDSEN (Alpine Multiscale Numerical Simulation Engine) software tool, for example for the specification of the snow albedo (Strasser et al., 2004). Such specification procedures involve tentative simulations that are evaluated by a comparison with observations. Best consistency of simulations and observations indicate an adequate value of a parameter. Parameters specified at a certain site are often transferred to other sites for want of better information.

Environmental data science can provide a remedy to the scarcity in site-specific parameters. The integration of data routinely gathered and delivered by monitoring systems (such as weather observations including snow depths) with data analysis tools facilitates the estimation of the wanted parameters for many locations and time periods. The results of the estimation procedure find their way into the operational snow forecasting for the benefit of the public. So far, in this chain of data flow there is a gap because of the lack of an adequate technique providing the site-specific parameters.

Taking advantage of the ESCIMO software code, here we suggest an inverse model for the estimation of model parameters from routinely observed snow data. Due to the complexity of the ESCIMO model, straightforward estimation techniques (e.g. maximum likelihood) are difficult to apply, and therefore we suggest Bayesian inference that provides interval estimates for the model parameters. In the following we explain the development, application and evaluation of this approach for the parameters snow density, snow albedo, snow emissivity, and soil heat flux. Compared to all other model parameters, these parameters are most influenced by the considered site. Parameters representing threshold values can weaken the convergence of the Markov Chain Monte Carlo simulations applied for the Bayesian inference. For that reason these threshold parameters will need special consideration and we did not include them here.

In our approach, the ESCIMO model was implemented, for parameter estimation, in OpenBUGS (Lunn et al., 2009) and, for simulations, also in R (R Core Team, 2014). In an extensive validation

119
120
121
122
123
124
125
126
127
128
129
130
131
132
133
134
135
136
137
138
139
140
141
142
143
144
145
146
147
148
149
150
151
152
153
154
155
156
157
158
159
160
161
162
163
164
165
166
167
168
169
170
171
172
173
174
175
176
177

study with simulated data we investigated the performance of the Bayesian parameter estimation and assessed bias and uncertainty of the estimates. Finally, the estimation procedure was applied to snow depth data observed at three different stations for a comparison of the estimated parameter values.

Our study region is Thuringia situated in the Central German Uplands. Analyzing meteorological data measured at the stations in Erfurt-Weimar (316 m a.s.l.), Artern (164 m a.s.l.), and Wasserkuppe (912 m a.s.l.), we probe ESCIMO at sub-alpine levels and with urban influences. All data were provided by the German Weather Service (DWD, Regionales Klimainformationssystem ReKIS). As the ESCIMO.spread model works with longwave radiation measurements in the energy balance and these data were unavailable from the considered stations, here we additionally suggest a parameterization scheme for the longwave radiation. The contribution of longwave radiation to the energy balance is parameterized by the snow emissivity, which is one of our estimated parameters. For compatibility with the observed meteorological data, for which hourly data were not available, we also modified the time-basis of ESCIMO from hourly to daily time-steps.

Exploring the capabilities and limitations of ESCIMO, in our study we hypothesize that:
- site-specific model parameters can be estimated by means of inverse modelling; they vary between sites and can differ from values given in the literature,
- for sub-alpine sites, the estimated parameters can improve the performance of ESCIMO compared to the default parameter values suggested with ESCIMO.spread in the alpine context,
- routinely gathered meteorological data are suitable for snow depth predictions based on ESCIMO utilizing parameter estimates derived from past snow observations, and this procedure of inverse modelling can be included into operational weather forecasting systems,
- site-specific parameter estimates suggest that the accumulation of snow depends on the altitude,
- ESCIMO is applicable to both hourly and daily meteorological data.

2   Model setup and inverse modelling

The energy balance (EB), equ.(5), of a snow pack is modelled considering the soil heat flux (B), advective energy (aS and aR, respectively) supplied by solid (S) or liquid (R) precipitation, sensible (H) and latent (E) heat fluxes, as well as short- ($(1-\alpha)G$) and longwave (L) net radiation. On the basis of the individual terms given in detail by (Strasser and Marke, 2010) the energy balance is applied to melting (if air temperature ≥ 273.15K) and no melt (air temperature < 273.15K) and eventually predicts the snow water equivalent (SWE in mm). Here the model was reformulated for the random variable snow depth ($SD = \frac{SWE}{10} \cdot \frac{\rho_W}{\rho_o}$ in cm with the density of water ρ_W) that involves the station specific snow densities (in units of $\rho_W = 1g/cm^3$; ρ_o for new snow, ρ_M for melting snow, ρ_s for sublimated snow, and ρ_r for frozen rain on snow cover) and is assumed to follow an exponential distribution.

Altogether, our hierarchical statistical model is

$$SD_t \sim \exp(\lambda_t), \qquad f_{\exp}(x,\lambda) = \begin{cases} e^{-x/\lambda}/\lambda & \text{for} \quad x \geq 0 \\ 0 & \quad x < 0 \end{cases}, \qquad E[x] = \lambda, \text{var}[x] = \lambda^2 \qquad (1)$$

3

$$\lambda_t = \begin{cases} \max\left(0, SD_{t-1} + R_t/(10\rho_r) + S_t/(10\rho_o) + Sub_t/(10\rho_s) - Melt_t/(10\rho_M)\right) & for \quad SD_{t-1} > 0 \\ S_t/(10\rho_o) & \quad SD_{t-1} = 0 \end{cases} \qquad (2)$$

$$Sub_t = \begin{cases} 86400 \; E_t/283550 & for \quad SD_{t-1} > 0 \\ 0 & \quad SD_{t-1} = 0 \end{cases} \qquad (3)$$

$$Melt_t = \begin{cases} \min\left(86400 \; EB_t/337500, \; 10 \cdot \rho_M \cdot SD_{t-1}\right) & for \quad SD_{t-1} > 0 \;\; and \;\; EB_t > 0 \\ 0 & \quad otherwise \end{cases} \qquad (4)$$

$$EB_t = B + aS_t + aR_t + H_t + E_t + (1-\alpha)G_t + L_t(\varepsilon_s) \qquad (5)$$

$$B = 2.0 \qquad (6)$$

$$aS_t = \begin{cases} \vartheta_t \cdot 2100 \cdot S_t/86400 & for \quad S_t > 0 \\ 0 & \quad S_t = 0 \end{cases} \qquad (7)$$

$$aR_t = \begin{cases} \vartheta_t \cdot 4180 \cdot R_t/86400 & for \quad R_t > 0 \\ 0 & \quad R_t = 0 \end{cases} \qquad (8)$$

$$H_t = 18.85\,(a+b\cdot u_t)\,(\vartheta_t - \vartheta_{St}), \qquad\qquad \vartheta_{St} = \min(\vartheta_t, 0) \qquad (9)$$

$$E_t = 32.82\,(a+b\cdot u_t)\,(e_t - e_{St}), \quad e_t = E(\vartheta_t)\cdot relHum_t, \quad e_{St} = \begin{cases} E(\vartheta_t) & for \quad SD_t > 0 \\ 0 & \quad SD_t = 0 \end{cases} \qquad (10)$$

$$L_t = ((1-s_t) + \varepsilon_{cl,t} s_t)\cdot 5.67\cdot 10^{-8}\cdot(\vartheta_t + 273.16)^4 - \varepsilon_s\cdot 5.67\cdot 10^{-8}\cdot(\vartheta_{St} + 273.16)^4, \qquad (11)$$

$$s_t = G_t/I_t, \qquad\qquad \varepsilon_{cl,t} = 1 - (1 + 4650\tfrac{e_t}{\vartheta_t+273.16})\exp(-(1.2 + 3*4650\tfrac{e_t}{\vartheta_t+273.16})^{0.5}) \qquad (12)$$

The expectation value of snow depth (λ) results from the sum of precipitation, sublimation and melting depending on whether there was snow cover on the previous day (eq. 2). For days without snow cover both sublimation and melting disappear (eqs. 3+4). In case of snow cover the water equivalent of sublimation (Sub, eq. 3) is determined by the available latent heat (E, eq 10) which in turn depends on the relative humidity ($relHum$) and convection due to wind speed (u). Equation (3) couples the latent heat (in W/m²) to the amount of sublimated snow (in mm/(86400 s)) by help of the sublimation heat of water (283550 Ws/kg). Likewise, eq. (4) couples the energy balance (eq. 5) to the amount of melted snow by help of the melting heat of snow (337500 Ws/kg). While eq. (2) represents the mass balance, eq. (5) is the energy balance and both are linked via sublimation and melting (eqs. 3 and 4). Melting (eq. 4) occurs only when the energy balance (EB, eq. 5) is positive, i.e. the energy flux is directed to the surface (all energy flux densities are expressed in W/m²). Melting is limited either by the available amount of snow or by the available energy (eq. 4).

In the model ESCIMO.spread a constant soil heat flux of $B = 2W/m^2$ was assumed (eq. 6), as soil heat flux measurements are scarcely available. The advective energy supplied by snow or by rainfall on snow is proportional to the amount of precipitation, the air temperature, and the specific heat of snow ($c_s = 2100 Jkg^{-1}K^{-1}$) or water ($c_w = 4200 Jkg^{-1}K^{-1}$), respectively (see eqs. 7+8,

4

86400 representing the number of seconds per day). The sensible heat flux (H) is expressed with wind speed (u in m/s) in eq. (9) and, accordingly, the latent heat flux (E) is calculated in eq. (10) where (e in hPa) is the water vapor partial pressure calculated using the Magnus formula ($E(\vartheta)$), and e_s likewise for the snow surface (Kuchment and Gelfan, 1996). The last but one term in the energy balance (eq. 5) represents the amount of shortwave radiation (global radiation, G in $J/cm^2 = 8.64\,W/m^2$) which is absorbed by the snow surface with the parameter snow albedo (α).

Extending the ESCIMO model that requires measurements of the incoming longwave radiation, here we assess this term using the clear sky emissivity (ε_{cl}) for the fraction of sky not covered by clouds (eq. 11). For the clear sky emissivity we use an empirical formula (see Prata (1996)). The cloud fraction is estimated by help of the solar index (s, eq. 12) that is the ratio between measured global radiation and theoretical shortwave radiation (I_t) for clear sky conditions. This effective solar constant I_t involves the solar constant ($I_o = 1370\ W/m^2$), corrections by zenith angle (Z, with $\cos(Z) = \sin(\text{geographic latitude})\sin(\text{declination}) + \cos(\text{geographic latitude})\cos(\text{declination})\cos(h)$, hour angle $h = (\pi/12)(t_{noon} - t)$), $\text{declination} = 0.4102\sin(\frac{2\pi}{365}(DoY - 80))$, $DoY = \text{Day of the Year}$) and transmission coefficients (Crawford and Duchon, 1999): $I_t = I_o \cos(Z)T_R T_{pg} T_w T_a$. (13)

For the transmission coefficients we have (Atwater and Brown, 1974; McDonald, 1960; Meyers and Dale, 1983):

$$T_R T_{pg} = 1.021 - 0.084\ \sqrt{m\,(0.00949\ p + 0.051)}\,, \qquad m = 35\cos(Z)\big/\sqrt{1224\cos^2(Z)+1}\,, \qquad (14)$$

$$T_w = 1 - 0.077(w\,m)^{0.3},\ T_a = 0.935^m \quad \text{with} \qquad\qquad (15)$$

air pressure p in kPa, optical air mass m at $101.3\,\text{kPa}$, precipitable water $w = 4650\ e/T$ for e as vapor pressure in kPa and T as air temperature in K. In the longwave radiation balance (eq. 11), incoming radiation is complemented by outgoing radiation parameterized by snow emissivity (ε_s).

A second extension of the ESCIMO model, which calculates the snow water equivalent (SWE in mm), is the conversion into snow depth (SD) that involves the station-specific snow density (for new snow an approximation is $\rho_0 = 0.05\ g/cm^3$, see glossar at www.dwd.de). This is taken into account in eq. (2). Thirdly, while the original ESCIMO was working on an hourly basis (t in h), here we used the model for daily observations (for that purpose the 86400 s (representing one day) were included in eqs. 3, 4, 7, and 8) and the meaning of all quantities changed accordingly (t in d). In the calculation of the effective solar constant (eq. 13) we used $t = t_{noon}$.

The ESCIMO model was implemented in R for the calculation of simulations and, additionally, in OpenBUGS (Lunn et al., 2009) applying an MCMC (Markov Chain Monte Carlo) scheme (based on the Gibbs sampler) for Bayesian inference. Table 1 summarizes all observational variables, the parameters and the constants of the ESCIMO model (eqs. 1-12). For the inverse modelling of the parameters snow density, snow albedo, snow emissivity, and soil heat flux we utilized flat priors of uniform, uniform, uniform, and exponential distributions, respectively.

Table 1: Variables, parameters, and constants of ESCIMO (eqs. 1-12) used for simulations and validation.

variable	symbol					unit
Snow depth	SD					cm
Precipitation as snow	S					mm
Precipitation as rain	R					mm
Wind speed	u					m/s
Air temperature	ϑ					$°C$
Relative air humidity	$relHum$					$\%$
Global radiation	G					$W\,m^{-2}$
parameter	symbol	default	Wasserk.	Erfurt-W.	Artern	unit
Albedo	α	0.90	0.90	0.90	0.90	--
Density of snow	ρ_o	0.05	0.18	0.13	0.10	g/cm^3
Emissivity of snow	ε_S	0.99	0.99	0.99	0.99	--
Soil heat flux	B	2.00	2.00	2.00	2.00	$W\,m^{-2}$
Threshold temperature for precipitation phase detection	T_w	275.16				K
constant	symbol	value				unit
Stefan-Boltzmann constant	σ	5.67×10^{-8}				$W\,m^{-2}K^{-4}$
Specific heat of snow (at 0°C)	c_{ss}	2.10×10^{3}				$J\,kg^{-1}K^{-1}$
Specific heat of water (at 5°C)	c_{sw}	4.20×10^{3}				$J\,kg^{-1}K^{-1}$
Melting heat of ice	c_i	3.337×10^{5}				$J\,kg^{-1}$
Sublimation/resublimation heat of snow (at -5°C)	l_s	2.8355×10^{6}				$J\,kg^{-1}$

3 Design of the study

In a first step, daily snow depths were simulated for different values of the considered four parameters (snow density in a range of $\rho_o = \rho_M = \rho_r = \rho_s \Rightarrow \rho = 0.1(0.01)0.2$, snow albedo in a range of $\alpha = 0.1(0.1)0.9$, snow emissivity in a range of $\varepsilon_s = 0.90(0.01)0.99$, and soil heat flux in a range of $B = 1.5(0.1)2.5$) and using real meteorological data at three sites (Erfurt-Weimar, Artern, Wasserkuppe) for a 2.5-year period (August 2010 – December 2012).

Applying the Bayesian inversion procedure (see OpenBUGS code in supporting material) to these simulated data, we calculated estimates for the specified four parameters. Finally, we compared the estimates with the original parameter values used in the simulations. From this validation the precision of the estimates and the occurrence of biases become obvious. Biases can result from dependencies between parameters. As most of the parameters are tied in with eq. (5) we speculate that the parameter estimates might be biased in some combinations and for some values. Analyzing the mutual interaction of parameters, we estimated them in all 32 different combinations (α in combination with others: $(\alpha);(\alpha,B);(\alpha,\rho);(\alpha,\varepsilon_s);(\alpha,\rho,B);(\alpha,\rho,\varepsilon_s);(\alpha,\varepsilon_s,B);(\alpha,\varepsilon_s,B,\rho)$;

ρ in combination with others: $(\rho);(\rho,B);(\rho,\alpha);(\rho,\varepsilon_s);(\rho,\alpha,B);(\rho,\alpha,\varepsilon_s);(\rho,\varepsilon_s,B);(\rho,\varepsilon_s,B,\alpha)$;

B in combination with others: $(B);(B,\rho);(B,\alpha);(B,\varepsilon_s);(B,\alpha,\rho);(B,\alpha,\varepsilon_s);(B,\varepsilon_s,\rho);(B,\varepsilon_s,\rho,\alpha)$;

ε_s in combination with others: $(\varepsilon_s);(\varepsilon_s,B);(\varepsilon_s,\alpha);(\varepsilon_s,\rho);(\varepsilon_s,\alpha,B);(\varepsilon_s,\alpha,\rho);(\varepsilon_s,\rho,B);(\varepsilon_s,\rho,B,\alpha)$)

keeping the other parameters constant, respectively. For the constant parameters we used the ESCIMO default values (Table 1). The MCMC procedure run for 100.000 updates (thinning 100) with rapid convergence (Fig. 1) for $\alpha, \rho, \varepsilon_s$. For B the convergence was much poorer. All results were robust against variations in the start values.
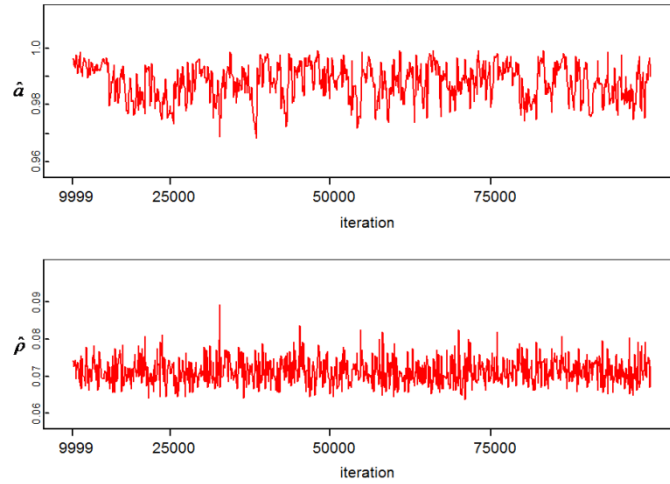
Figure 1: Convergence of MCMC iterations for an estimation of albedo and snow density with OpenBUGS (using data at Erfurt-Weimar; results are similar for the other stations).

After model validation we applied the approach to observational data gathered routinely at three weather stations (Erfurt-Weimar, Artern, Wasserkuppe) and estimated the four parameters $(\alpha, \varepsilon_s, B, \rho)$ well as their uncertainty for different parameter combinations. All results were robust against variations in the start values. The performance of the estimation procedure was finally assessed from the quality of forecasts calculated with observed data for a 51-years period (sect. 4.3).

4   Results

4.1 Model validation

Validating the suggested inverse modelling procedure we compared parameter estimates with the parameter values used for simulating the data. This comparison also considered joint estimations of different parameter combinations for an assessment of mutual bias effects (See Fig. 2 for Wasserkuppe; results are similar for stations Erfurt-Weimar and Artern).

A feature that is obvious for all three stations is the occurrence of a strong bias towards larger albedo estimates if the albedo is estimated together with the snow emissivity. In contrast, snow density and soil heat flux do not bias the albedo estimate. The dependence between the estimates $\hat{\alpha}$ and $\hat{\varepsilon}_s$ is a consequence of eq. (5) where the albedo is a coefficient of global radiation (G) and snow emissivity is a coefficient of the surface temperature (ϑ_s, see eq. 11). A quantitative comparison of the terms in eq. (5) reveals that for large albedo ($\alpha > 0.9$) the short- and the longwave energies are similar. During clear sky conditions the radiation and surface temperature data are collinear and this generates an association between the estimates $\hat{\alpha}$ and $\hat{\varepsilon}_s$. Further, we find that the bias of $\hat{\alpha}$ is

414
415
416
417
418
419
420
421
422
423
424
425
426
427
428
429
430
431
432
433
434
435
436
437
438
439
440
441
442
443
444
445
446
447
448
449
450
451
452
453
454
455
456
457
458
459
460
461
462
463
464
465
466
467
468
469
470
471
472

largest for Wasserkuppe and smallest for Artern. This might be caused by different ageing of snow due to differences in altitude (ca. 800m) and shortwave radiation.
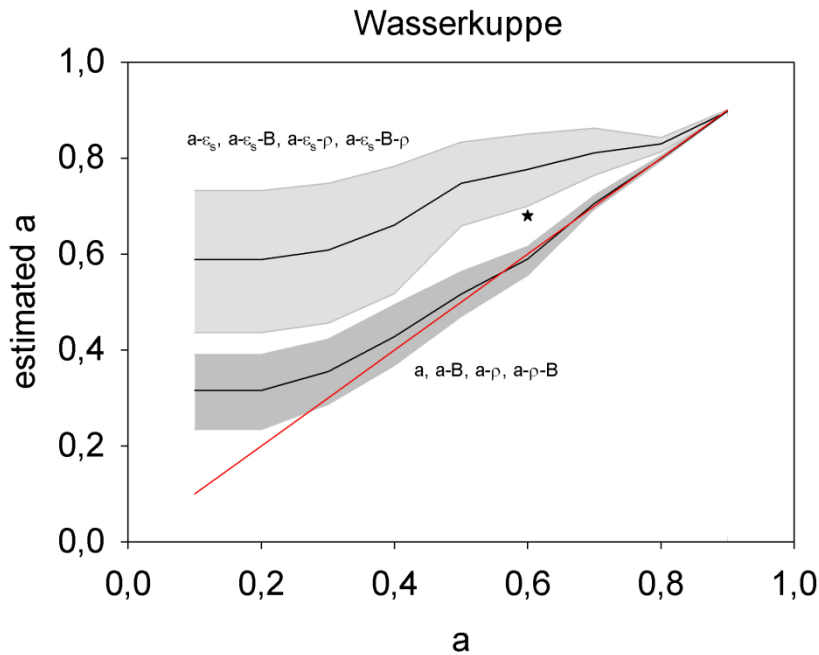
Figure 2: Estimated albedo at station Wasserkuppe (for $\varepsilon_s = 0.99, \; B = 2.0 \, W / m^2, \; \rho = 0.18 g / cm^3$) depending on the albedo used for snow depth simulation and on the combination of parameter estimates. Dark lines represent the median; grey areas range from 25th to 75th percentile; red line indicates exact correspondence. All estimates cluster in two distinct groups of error ranges; the group involving snow emissivity is strongly biased to larger albedo estimates. The asterisk represents the median albedo estimated for a simulation using $\varepsilon_s = 0.9, \; \alpha = 0.6$.

In our validation study we simulated snow depth data for $\varepsilon_s = 0.99$, which is too large (compared with the real snow emissivity estimated for Wasserkuppe; see below) and therefore the albedo is overestimated. Testing a more realistic value of $\varepsilon_s = 0.90$ for simulations, the bias of the estimated albedo (jointly estimated with ε_s) is clearly reduced (cf. asterisk in Fig. 2). This finding suggests that for subalpine regions the default $\varepsilon_s = 0.99$ in ESCIMO might have to be replaced by a more adequate value. Later on we will recommend values for ε_s on the basis of a joint estimation of albedo and snow emissivity from observational data (see below).

Another clear and general feature is that the error range of the albedo estimate decreases with increasing albedo. Estimations become more precise with the availability of more data that means for long spells of snow, which can be generated by repeated snow fall. In this way, long spells represent the large albedo of fresh snow ($\alpha \approx 0.8 - 0.9$, (Kraus, 2008)). Conversely, short spells of snow-cover can represent aged snow ($\alpha \approx 0.45 - 0.90$, (Kraus, 2008)).

Comparing the different stations we observed that the albedo estimates equal the theoretical albedo only for values larger than approximately 0.5. For $\alpha < 0.5$ the error increases and for very small albedo values the estimate is nearly independent on the albedo used for the simulations (this is obvious for the stations Erfurt-Weimar and Artern; not shown here). This can be understood as a consequence of the differences in the number of days without snow that is $92\%, 89\%, 75\%$ in the

8

473
474
475
476
477
478
479
480
481
482
483
484
485
486
487
488
489
490
491
492
493
494
495
496
497
498
499
500
501
502
503
504
505
506
507
508
509
510
511
512
513
514
515
516
517
518
519
520
521
522
523
524
525
526
527
528
529
530
531

considered time period for Artern, Erfurt-Weimar, and Wasserkuppe, respectively. For large albedo values ($\alpha \geq 0.90$) the bias vanishes for all stations, even for the albedo estimated jointly with snow emissivity, and the error range diminishes to about 1%. For small albedo values ($\alpha < 0.50$) the estimation is strongly biased and therefore useless.

Though the estimates of the snow density (ρ) tend to be slightly biased by a joint estimation together with snow emissivity (Figure 3), this bias is not significant because the error range includes the exact agreement between theoretical and estimated values. There is a general (but also not significant) tendency to overestimate the snow density. As Wasserkuppe has more days with snow cover, the precision of the estimated snow density is higher, compared with the other stations.
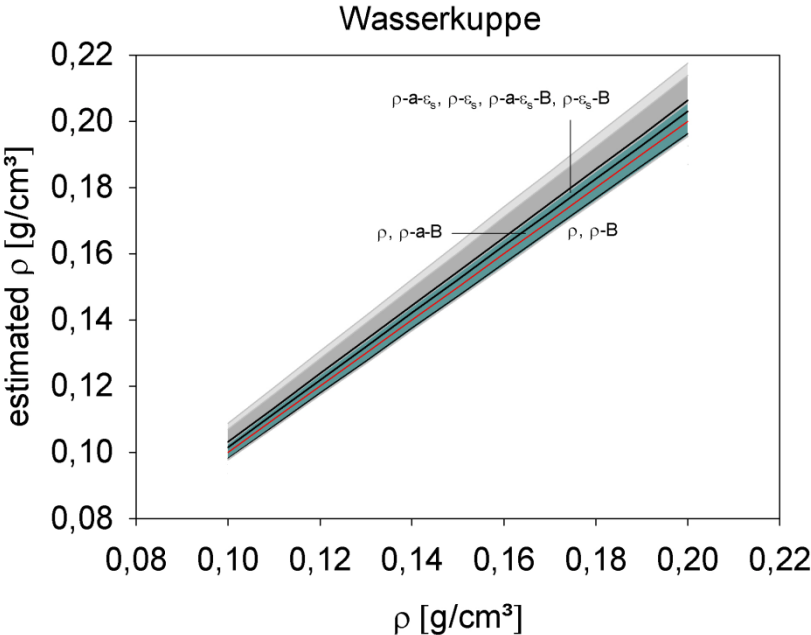
Figure 3: Estimated snow density at station Wasserkuppe (for $\alpha = 0.90,\ \varepsilon_s = 0.99,\ B = 2.0\,W/m^2$) depending on the snow density used for snow depth simulation and on the combination of parameter estimates. Dark lines represent the median; grey areas range from 25th to 75th percentile; red line represents exact correspondence.

The estimation of snow emissivity (ε_s) has diverse results (Fig. 4). For Wasserkuppe all estimates cluster in three distinct groups (Figure 4a). A joint estimation of ε_s with albedo generates an overestimation and an estimation jointly with snow density (but not with albedo!) generates an underestimation of the snow emissivity in the range $0.95 < \varepsilon_s < 0.96$. For Erfurt-Weimar just those estimations involving the albedo, are biased towards larger snow emissivity and all others are unbiased (Figure 4b). For the station Artern all estimations of snow emissivity are nearly not biased (Figure 4c).

In result, for values $\varepsilon_s > 0.92$ the estimation of snow emissivity is free of bias. Our simulations confirm the above observation that estimates of albedo and snow emissivity interact. Therefore the accuracy of snow emissivity estimations might be improved for other values of the albedo.
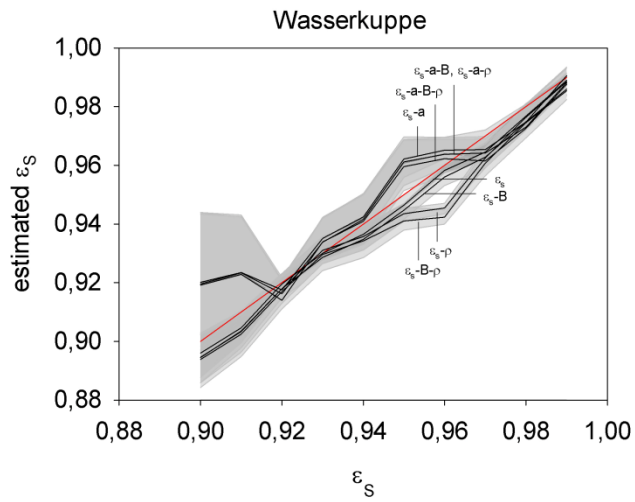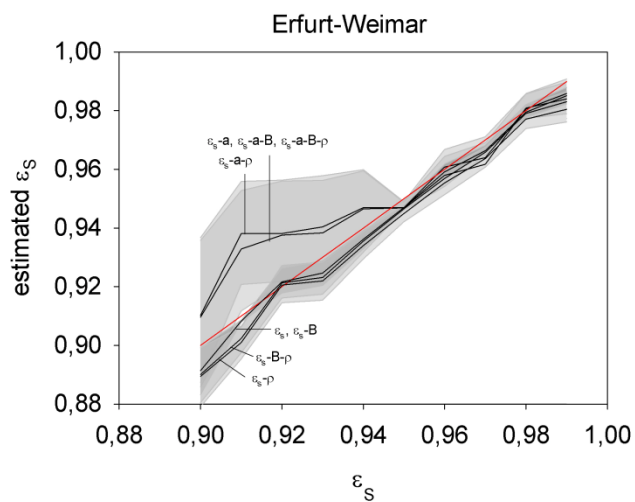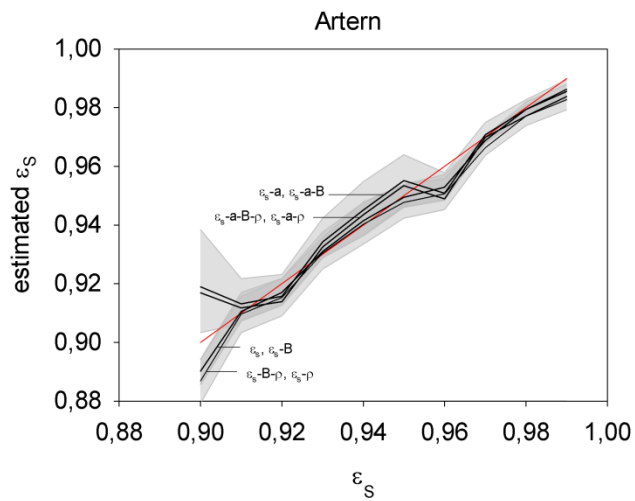
Figure 4: Estimated snow emissivity at Wasserkuppe (a, for $\rho = 0.18\,g/cm^3$), Erfurt-Weimar (b, for $\rho = 0.13\,g/cm^3$), and Artern (c, for $\rho = 0.10\,g/cm^3$) (all with $\alpha = 0.90,\;\; B = 2.0\,W/m^2$) depending on the snow emissivity used for snow depth simulation and on the combination of parameter estimates. Dark lines represent the median; grey areas range from 25th to 75th percentile; red line represents exact correspondence.

To illustrate an advantage of the Bayesian approach over the maximum likelihood method we used the latter for the estimation of the parameter snow emissivity (ε_s). For the estimation of this parameter and the situation of snow cover ($SD > 0$) and without any snow or rain precipitation ($S = R = 0$) the ESCIMO equations can be reformulated to a generalized regression. This regression with offset involves an exponential distribution of the snow depth $SD_t \sim \exp(\lambda_t)$. Given $\rho = 0.1 g/cm^3$ and the daily values of $SD_t, \vartheta_t, relHum_t, u_t$, an estimate of the snow emissivity can be calculated e.g. in R using glm (with Gamma distribution as generalization of the exponential and with inverse link function) and results in $\hat{\varepsilon}_s = 1.11 \pm 0.14 \in [0.97, 1.25]$ for the station Wasserkuppe. This interval estimate overlaps with the Bayesian estimate 0.99 ± 0.01, but does not comply with the restriction $0 \leq \varepsilon_s \leq 1$, as maximum likelihood estimators approximately follow a normal distribution.

The estimation of the soil heat flux (B) is rather poor (Figure 5) for all stations. There is not only bias but also a very large error range. The latter fact corresponds to the poor convergence of the MCMC procedure (not shown here) that has extremely extended the computing time. Considering the magnitude of the energy terms in the balance eq. (5), we find that B is smaller than all other terms by a factor of 1/10 ... 1/100. Therefore minor inaccuracies of the other energy terms will have an immense impact on the estimation of the soil heat flux.
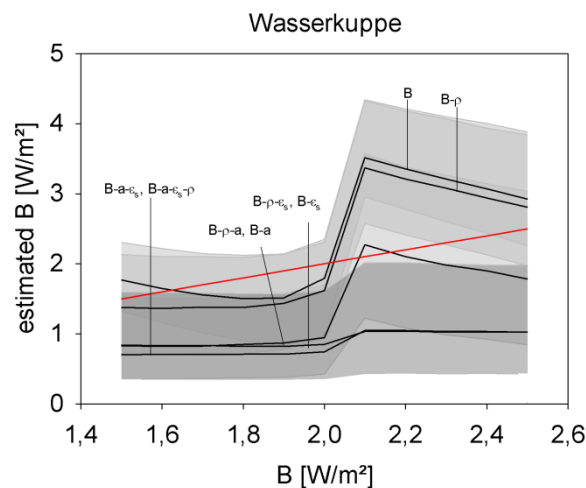
Figure 5: Estimated soil heat flux at station Wasserkuppe (for $\alpha = 0.90,\ \rho = 0.18 g/cm^3,\ \varepsilon_s = 0.99$) depending on the soil heat flux used for snow depth simulation and on the combination of parameter estimates. Dark lines represent the median; grey areas range from 25th to 75th percentile; red line represents exact correspondence.

Another reason for the large estimation error of B is that the soil temperature that is relevant for the soil heat flux can be different. ESCIMO assumes a soil temperature equal to the snow temperature (of 273.15K), and this is just an approximate parameterization of the model. Further, the bias of the soil heat flux estimate towards lower values might be caused by the fact that we use the ESCIMO equations for daily time-steps. Originally it was designed for hourly time-steps and was able to account for reduced soil heat fluxes during the night. This makes the daily average soil heat flux smaller than the flux during the day-time.

Summarizing our validation study of all the four considered parameters, we conclude that snow density is estimated most accurately and this is in agreement with the good convergence of the

11

650
651
652
653
654
655
656
657
658
659
660
661
662
663
664
665
666
667
668
669
670
671
672
673
674
675
676
677
678
679
680
681
682
683
684
685
686
687
688
689
690
691
692
693
694
695
696
697
698
699
700
701
702
703
704
705
706
707
708

MCMC simulation (Figure 1). In contrast, the estimation of soil heat flux is very poor. Albedo and snow emissivity estimates interact and this suggests making a joint estimation in order to have reasonable values for both.

4.2 Model application to observational data

In an application of the suggested inverse modelling procedure, we estimated the four parameters (α, ρ, ε_s, B) from real snow depth data recorded at three stations. For each station all parameters have been estimated in different combinations. At the beginning, each parameter was estimated alone and the other parameters were set to fixed values. This was completed by pairs and triples of parameter estimates; finally all four parameters were estimated jointly and this procedure resulted in consistent estimates.

Extending the original ESCIMO model that calculates the snow water equivalent (SWE), here we directly modelled the snow depth (SD). In the application study we observed that the ratio SWE/SD significantly depends on the state of the snow cover and, therefore, we included different snow densities for new snow (ρ_o), for melting snow (ρ_M), for sublimated snow (ρ_s), and for frozen rain on snow cover (ρ_r) into the mass balance (eq. 2). All snow densities are limited in their value by the density of ice that is $\rho_{ice} = 0.918\, g/cm^3$ and this was taken into account in the inverse modelling approach. Joint estimations of the four densities always resulted in $\hat{\rho}_s = \hat{\rho}_r = \hat{\rho}_M = \rho_{ice}$. Generally the estimated density of new snow is lower than for ice ($\hat{\rho}_o < \rho_{ice}$); even for aged snow covered by firn or ice the density is below $0.6\, g/cm^3$.

Estimating from our observational data the density of new snow (Tab. 2) we found station-specific values of $\hat{\rho}_o \approx 0.14\, g/cm^3$ and $\hat{\rho}_o \approx 0.05\, g/cm^3$ for Wasserkuppe and Erfurt-Weimar, respectively. For Artern the snow density was consistently estimated as $\hat{\rho}_o \approx 0.11\, g/cm^3$. Obviously, the snow density increases with the accumulation and ageing of snow and this occurs more likely at a mountain station (Wasserkuppe) as opposed to an urban lowland station (Erfurt-Weimar) where the time of snow cover is reduced due to urban heat island effects.

The snow emissivity $\hat{\varepsilon}_s$ varies between stations (Table 2). The estimation of the soil heat flux $\hat{B}$ was very uncertain as a consequence of the dominance of the other parts in the energy balance. Nevertheless, our estimations indicated that a value of $\hat{B} \approx 1.0 W/m^2$ is reasonable for the soil heat flux in our study region; the default value in ESCIMO is $2.0\ W/m^2$. All achieved estimates are summarized in Table 2 as a recommendation for the application of ESCIMO with data relevant for subalpine regions.

The estimated albedo was site specific and decreased from Wasserkuppe ($\hat{\alpha} \approx 0.94$) to Erfurt-Weimar ($\hat{\alpha} \approx 0.89$) to Artern ($\hat{\alpha} \approx 0.56$). These changes in the albedo correspond to the changes in the altitude of these stations ($921\,m, 316\,m, 164\,m$) a.s.l.. Stations at higher altitudes experience new snowfall more often and this is associated with a larger albedo. Strasser and Marke (2010) used albedo values between 0.45 and 0.90. Combining albedometer measurements with Landsat TM images for an alpine glacier, Strasser et al. (2004) developed a parameterization of the albedo

12

$\alpha = \alpha_{min} + \alpha_{add} \cdot e^{-kn}$ with n representing the number of days since the last considerable snowfall (i.e. at least $SWE = 0.5\ mm/h$) which causes an increase of the snow albedo to its maximum value $\alpha_{min} + \alpha_{add}$ (α_{min} is the minimum albedo of (old) snow, α_{add} is an additive albedo and k is a recession factor that is defined as -0.12 for positive temperatures and -0.05 for negative temperatures, (Strasser and Marke, 2010)).

This parameterization was also used in ESCIMO and specifies the maximum albedo to 0.95, but this level can be clearly exceeded by fresh snow in alpine regions (Fig. 17 in Strasser et al. (2004)). Our results for sub-alpine stations suggested that the albedo was often below this level. We also found that for our stations an ageing model for albedo changes was not significant (Tab. 2).

Table 2: Parameter values jointly estimated from measured snow depth data (generally $B = 1\ W/m^2$, and $\rho_s = \rho_r = \rho_M = 0.918\ g/cm^3$,)

Parameter estimated	Wasserkuppe (921 m a.s.l.)	Erfurt-Weimar (316 m a.s.l.)	Artern (164 m a.s.l.)
$\hat{\alpha}$	0.94±0.04	0.89±0.05	0.56±0.04
$\hat{\alpha}_{min}$; $\hat{\alpha}_{add}$	0.93±0.05; 0.03±0.03	0.89±0.08; 0.04±0.06	0.52±0.06; 0.05±0.05
$\hat{\rho}_o\ [g/cm^3]$	0.14±0.02	0.05±0.01	0.11±0.02
$\hat{\varepsilon}_s$	0.88±0.01	0.92±0.03	0.99±0.01

An important observation is that the albedo estimation is based on the energy balance (eq. 5) of the ESCIMO model and this energy balance is involved merely in the amount of melting snow (eq. 4). That means albedo estimates are calculated only from observational data that refer to melting and, therefore, $\hat{\alpha}$ is the albedo of melting snow! For new snow an estimation of α is not possible using the ESCIMO approach. This fact explains the unexpected small values of $\hat{\alpha}$ and the insignificance of the snow ageing obtained from our observational data.

4.3 Performance assessment

Assessing the quality of the parameters estimated by an inverse modelling of the 2.5 years observational data, we used them to calculate predictions for 2.5-years and 51-years periods. While the former demonstrates the precision of model fit, the latter represents the model's ability for generalization. We applied the following performance measures:

coefficient of determination $R^2 = \left(\dfrac{\sum_{t=1}^{n}\left(SD_t^{(obs)} - \overline{SD^{(obs)}}\right) \cdot \left(SD_t^{(mod)} - \overline{SD^{(mod)}}\right)}{\sqrt{\sum_{i=1}^{n}\left(SD_i^{(obs)} - \overline{SD^{(obs)}}\right)^2} \cdot \sqrt{\sum_{k=1}^{n}\left(SD_k^{(mod)} - \overline{SD^{(mod)}}\right)^2}} \right)^2$,

index of agreement $IA = 1 - \dfrac{\sum_{t=1}^{n}\left(SD_t^{(obs)} - SD_t^{(mod)}\right)^2}{\sum_{i=1}^{n}\left(\left|SD_i^{(mod)} - \overline{SD^{(obs)}}\right| + \left|SD_i^{(obs)} - \overline{SD^{(obs)}}\right|\right)^2}$, and root means square error

$RMSE = \sqrt{(1/n)\sum_{t=1}^{n}\left(SD_t^{(obs)} - SD_t^{(mod)}\right)^2}$, mean absolute error $MAE = (1/n)\sum_{t=1}^{n}\left|SD_t^{(obs)} - SD_t^{(mod)}\right|$, mean

bias error $MBE = (1/n)\sum_{t=1}^{n}\left(SD_t^{(obs)} - SD_t^{(mod)}\right)$, fractional bias error $FBE = \dfrac{\sum_{t=1}^{n}\left(SD_t^{(obs)} - SD_t^{(mod)}\right)}{0.5 \cdot \sum_{i=1}^{n}\left(SD_i^{(obs)} + SD_t^{(mod)}\right)}$.

While R^2 measures the percentage of variance in observed snow depths explained by the statistical model, the R^2 is not able to assess a bias between observed and predicted data (Willmott, 1982; Willmott et al., 1985). For a more comprehensive evaluation we included the index of agreement ($IA \in (0,1)$) that indicates a perfect prediction for $IA = 1$. MAE, MBE, and FBE indicate systematic errors. Default parameters in ESCIMO are $\alpha = 0.90, \varepsilon_s = 0.99, \rho = 0.10 \text{g/cm}^3, B = 2.0 W/m^2$.

Comparatively, the parameter values achieved from the Bayesian estimation procedure (summarized in Table 2) were used for snow depth predictions and an assessment of their quality (Table 3).

Table 3: Performance measures of forecasts based on different sets of parameters (default values are used to forecast the 2.5-years period in the first three lines; Bayesian estimates are used in light grey lines to predict the 2.5-years period and in dark grey lines for the 51-years period).

	R^2	IA	$RMSE$	MAE	MBE	FBE
Wasserkuppe; default parameters; 2.5 years $\alpha = 0.90,\ \rho_M = \rho_r = \rho_s = 0.918\,\text{g/cm}^3,$ $\rho_o = 0.05\text{g/cm}^3, \varepsilon_s = 0.99,\ B = 2.0\,W/m^2$	0.324	0.0896	259	159	-159	-1.85
Erfurt-Weimar; default parameters; 2.5 years $\alpha = 0.90,\ \rho_M = \rho_r = \rho_s = 0.918\,\text{g/cm}^3,$ $\rho_o = 0.05\text{g/cm}^3, \varepsilon_s = 0.99,\ B = 2.0\,W/m^2$	0.634	0.303	41.7	16.1	-16.1	-1.68
Artern; default parameters; 2.5 years $\alpha = 0.90,\ \rho_M = \rho_r = \rho_s = 0.918\,\text{g/cm}^3,$ $\rho_o = 0.05\text{g/cm}^3, \varepsilon_s = 0.99,\ B = 2.0\,W/m^2$	0.64	0.312	20.6	6.98	-6.98	-1.63
Wasserkuppe; Table 2; 2.5 years $\alpha = 0.94,\ \rho_M = \rho_r = \rho_s = 0.918\,\text{g/cm}^3,$ $\rho_o = 0.14\,\text{g/cm}^3, \varepsilon_s = 0.88,\ B = 1.0\,W/m^2$	0.631	0.608	30.8	13.9	-12.8	-0.989
Erfurt-Weimar; Table 2; 2.5 years $\alpha = 0.89,\ \rho_M = \rho_r = \rho_s = 0.918\,\text{g/cm}^3,$ $\rho_o = 0.05\,\text{g/cm}^3, \varepsilon_s = 0.92,\ B = 1.0\,W/m^2$	0.73	0.404	31.7	11.3	-11.2	-1.57
Artern; Table 2; 2.5 years $\alpha = 0.56,\ \rho_M = \rho_r = \rho_s = 0.918\,\text{g/cm}^3,$ $\rho_o = 0.11\,\text{g/cm}^3, \varepsilon_s = 0.99,\ B = 1.0\,W/m^2$	0.845	0.801	4.34	1.02	-0.804	-0.678
Wasserkuppe; Table 2; 51 years $\alpha = 0.94,\ \rho_M = \rho_r = \rho_s = 0.918\,\text{g/cm}^3,$ $\rho_o = 0.14\,\text{g/cm}^3, \varepsilon_s = 0.88,\ B = 1.0\,W/m^2$	0.578	0.591	32.4	13.4	-12.1	-0.917
Erfurt-Weimar; Table 2; 51 years $\alpha = 0.89,\ \rho_M = \rho_r = \rho_s = 0.918\,\text{g/cm}^3,$ $\rho_o = 0.05\,\text{g/cm}^3, \varepsilon_s = 0.92,\ B = 1.0\,W/m^2$	0.56	0.33	17.3	5.41	-5.34	-1.51
Artern; Table 2; 51 years $\alpha = 0.56,\ \rho_M = \rho_r = \rho_s = 0.918\,\text{g/cm}^3,$ $\rho_o = 0.11\,\text{g/cm}^3, \varepsilon_s = 0.99,\ B = 1.0\,W/m^2$	0.709	0.782	2.91	0.709	-0.46	-0.557

827
828
829
830
831
832
833
834
835
836
837
838
839
840
841
842
843
844
845
846
847
848
849
850
851
852
853
854
855
856
857
858
859
860
861
862
863
864
865
866
867
868
869
870
871
872
873
874
875
876
877
878
879
880
881
882
883
884
885

We found that the performance was clearly improved for the parameter values estimated by the suggested Bayesian procedure, referring to the 2.5-years period. Predictions for the 51-years period were slightly less precise. A conclusion is that the parameter estimation can be recommended for each specific site before ESCIMO is used to forecast the snow depth at this site. The sensitivity of forecasting performance on the soil heat flux was very low.

5   Conclusions and limitations

The ESCIMO model was utilized for an inverse approach assessing the model parameters on the basis of meteorological data gathered at three stations situated in the Central German Uplands. Referring to our research hypotheses, we conclude that the inverse modelling is suitable to estimate the model parameters for sub-alpine sites with urban influences and to calculate predictions of snow depth. Parameter values adequate for the low mountain range in Germany are summarized in Table 2 and are recommended for use in similar subalpine regions.

Extending the ESCIMO code from the snow water equivalent to the snow depth, we introduced the snow densities that need to be estimated. These additional parameter estimations are required because routine measurements provide just snow depths and the snow density can vary in time and space. Observational data of snow density are rare and therefore an advantage of the Bayesian approach is the possibility to assess this parameter specifically for each station. This estimate provides valuable information about site-specific conditions.

Our validation study clearly demonstrated how parameter estimates are mutually correlated and, therefore, a joint estimation of all parameters is recommended. This procedure guarantees that all parameter values are adequate to the prevailing state of the snow cover. The estimated site-specific parameters improve the performance of ESCIMO compared to the default parameter values suggested with ESCIMO.spread (see Table 3). The occurrence of site-specific values for the parameters suggested that the accumulation of snow depended on the altitude and the urban or mountain characteristic of a station.

Improvements are needed for the estimation of the soil heat flux. The parameterization applied here is rather simple and an involvement of the soil temperature profile might be beneficial. Possibly, the chosen exponential prior is not optimal and might be improved. A third problem to be solved with the estimation of B arises from its small value compared to the other terms in the energy balance.

Originally, ESCIMO was developed for hourly time steps (Strasser and Marke, 2010). For compatibility with observed meteorological data, for which only daily data are available, we modified the time-basis of ESCIMO from hourly to daily time-steps and this might have an impact on the interpretation of the parameter values. Especially the parameters $\alpha, \ \rho_o, \ \varepsilon_s, \ B$ studied here represent daily values, while, in the original ESCIMO code, they can vary during the day. This means, the parameters on a daily basis are certain averages of these hourly data and are attenuated in their extremes. For example, the ageing of snow appears smoothed in the daily parameters. Nevertheless, ESCIMO proved to be applicable to both hourly and daily data. As ESCIMO is a physically based point snow surface model, all estimated parameters refer to the location where the data have been gathered.

15

Our approach provides point values of snow density, albedo, snow emissivity, and soil heat flux. The model does not give any information about the changes of these parameters along the snow surface and with increasing distance to the observation site.

The extension of the original ESCIMO model by a parameterization of the long-wave radiation (eq. 11+12) proved to be beneficial, as this made the suggested inverse model applicable for routine monitoring data from which long-wave radiation is often not available. Including parameters for snow densities into the original ESCIMO model considerably improved the performance of the model because these parameters are mostly not available at the monitoring sites. Even the snow prediction for new datasets takes advantage of the parameters estimated by the suggested inverse model.

6   Software and data availability

The study is based on data gathered in the frame of the regional climate information system ReKIS. They were freely downloaded as text files from www.rekis.org for the stations Wasserkuppe, Erfurt-Weimar, and Artern as daily values for a period of 51 years (January 1st, 1961 until December 31st, 2012). For all calculations we used the free language R for statistical computing (www.r-project.org) in combination with the OpenBUGS software that is freely available at www.openbugs.net where all further information is provided. The code for the inverse model developed by the authors is provided in the supporting material.

7 Supporting material (OpenBUGS code for inverse ESCIMO model)

```
model
 {  for(i in 2:N){
                a[i]<-17.08085*(TM[i]-273.16)
                b[i]<-234.175+(TM[i]-273.16)
            DDL[i]<-6.1078*exp(a[i]/b[i])*(RF[i]/100)
             ObT[i]<-min(TM[i],273.16)
                c[i]<-17.08085*(ObT[i]-273.16)
                d[i]<-234.175+(ObT[i]-273.16)
            DDO[i]<-6.1078*exp(c[i]/d[i])
                  if_SWE1[i]<- 1-step(-SH[i-1])
                        DDO1[i]<- equals(if_SWE1[i],1)*DDO[i]
          e[i]<-0.18+0.098*FF[i]
          f[i]<-DDL[i]-DDO[i]
          latW[i] <- 32.82*e[i]*f[i]
          Sub[i] <- (86400*latW[i])/2835500
                  if_RR[i] <- 1-step(-(TM[i]-275.16))
                      R[i]<- equals(if_RR[i],1)*RR[i]

                  if_RR1[i] <- 1-step(-(TM[i]-275.16))
                        S[i]<- equals(if_RR1[i],0)*RR[i]

                  if_SWE[i] <- 1-step(-SH[i-1])
                    Sub1[i]<- equals(if_SWE[i],1)*Sub[i]

                  if_Schnee[i] <- 1-step(-S[i])
                    advekFS[i] <- equals(if_Schnee[i],1)*((TM[i]-273.16)*2100)*(S[i]/86400)

                  if_Regen[i] <- 1-step(-R[i])
                    advekFR[i] <- equals(if_Regen[i],1)*((TM[i]-273.16)*4180)*(R[i]/86400)

          g[i]<-0.18+0.098*FF[i]
          h[i]<-TM[i]-ObT[i]
          senW[i] <- 18.85*g[i]*h[i]
          Dekl[i] <- 0.4102*sin((2*3.141592654/365)*(DoY[i]-80))
          Zenit[i] <- sin(0.881356366)*sin(Dekl[i])+cos(0.881356366)*cos(Dekl[i])*cos(0)
          m[i] <- 35*cos(arccos(Zenit[i]))*pow(1224*pow(cos(arccos(Zenit[i])), 2)+1, -0.5)
          TransRaypG[i] <-  1.021-(0.084*sqrt((m[i]*(0.00949*P[i]+0.051))))
          PrecipWat[i] <- 4650*DD[i]/TM[i]
          TransWasser[i] <- 1-(0.077*(pow(m[i]*(PrecipWat[i]), 0.3)))
          TransAero[i] <- pow(0.935, m[i])
          cs_I[i] <- 1370*Zenit[i]*TransRaypG[i]*TransWasser[i]*TransAero[i]
          G8[i] <- GS[i]/8.64
          s[i] <-  G8[i]/cs_I[i]
          cs_Emi[i] <- 1-((1+PrecipWat[i])*exp(-sqrt(1.2+3*PrecipWat[i])))
          Bew_Emi[i] <- (1-s[i])+s[i]*cs_Emi[i]
          Inc_long_rad[i] <- 5.67*pow(10, -8)*Bew_Emi[i]*pow(TM[i], 4)
          longwave_rad_bal[i] <- Inc_long_rad[i] - Semmi*5.67*pow(10, -8)*pow(ObT[i], 4)
          EB[i] <-  (1-alb[i])*G8[i] + longwave_rad_bal [i]+ advekFS[i] + advekFR[i] + latW[i]
                            + senW[i] + B
          alb[i] <- amin + add*exp(-0.1*NN[i])
                  if_SWE2[i] <- 1- step(-SH[i-1]) - step(-EB[i])
                    Melt[i] <- equals(if_SWE2[i],1)*min(EB[i]*86400/337500, 10*rhom*SH[i-1])
                  if_SWE3[i] <- 1-step(-SH[i-1])
z[i] <- equals(if_SWE3[i],1)* max(10*SH[i-1]+R[i]/rhor+S[i]/rho0+Sub1[i]/rhos-Melt[i]/rhom,0)
+ (1-equals(if_SWE3[i],1))*  max(S[i]/rho0,0)
                  lambda[i] <- 1/((z[i]/10)+0.000001)
                  SH[i] ~ dexp(lambda[i])
                    }
        amin ~ dunif(0,1)
        add <- (1-amin)*aadd
        aadd ~ dunif(0,1)
        amax <- amin+add
        Semmi ~ dunif(0,1)
        B<-1.0
        rhor <- 0.918*rrhor
        rhos <- 0.918*rrhos
        rhom <- 0.918*rrhom
        rho0 <- 0.918*rrho0
        rrhor <- 1.0
        rrhos <- 1.0
        rrhom <- 1.0
        rrho0 ~ dunif(0,1)        }
```

8 References

Atwater, M.A., Brown, P.S., 1974. NUMERICAL COMPUTATIONS OF LATITUDINAL VARIATION OF SOLAR-RADIATION FOR AN ATMOSPHERE OF VARYING OPACITY. Journal of Applied Meteorology 13(2) 289-297.

Crawford, T.M., Duchon, C.E., 1999. An improved parameterization for estimating effective atmospheric emissivity for use in calculating daytime downwelling longwave radiation. Journal of Applied Meteorology 38(4) 474-480.

Kraus, H., 2008. Grundlagen der Grenzschicht-Meteorologie: Einführung in die Physik der Atmosphärischen Grenzschicht und in die Mikrometeorologie. Springer.

Kuchment, L.S., Gelfan, A.N., 1996. The determination of the snowmelt rate and the meltwater outflow from a snowpack for modelling river runoff generation. Journal of Hydrology 179(1-4) 23-36.

Lunn, D., Spiegelhalter, D., Thomas, A., Best, N., 2009. The BUGS project: Evolution, critique and future directions. Statistics in Medicine 28(25) 3049-3067.

McDonald, J.E., 1960. DIRECT ABSORPTION OF SOLAR RADIATION BY ATMOSPHERIC WATER VAPOR. Journal of Meteorology 17(3) 319-328.

Meyers, T.P., Dale, R.F., 1983. PREDICTING DAILY INSOLATION WITH HOURLY CLOUD HEIGHT AND COVERAGE. Journal of Climate and Applied Meteorology 22(4) 537-545.

Prata, A.J., 1996. A new long-wave formula for estimating downward clear-sky radiation at the surface. Quarterly Journal of the Royal Meteorological Society 122(533) 1127-1151.

R Core Team, 2014. R: A language and environment for statistical computing. R Foundation for Statistical Computing, Vienna, Austria.

Strasser, U., Corripio, J., Pellicciotti, F., Burlando, P., Brock, B., Funk, M., 2004. Spatial and temporal variability of meteorological variables at Haut Glacier d'Arolla (Switzerland) during the ablation season 2001: Measurements and simulations. Journal of Geophysical Research-Atmospheres 109(D3).

Strasser, U., Etchevers, P., Lejeune, Y., 2002. Inter-comparison of two snow models with different complexity using data from an alpine site. Nordic Hydrology 33(1) 15-26.

Strasser, U., Marke, T., 2010. ESCIMO.spread - a spreadsheet-based point snow surface energy balance model to calculate hourly snow water equivalent and melt rates for historical and changing climate conditions. Geoscientific Model Development 3(2) 643-652.

Willmott, C.J., 1982. SOME COMMENTS ON THE EVALUATION OF MODEL PERFORMANCE. Bulletin of the American Meteorological Society 63(11) 1309-1313.

Willmott, C.J., Ackleson, S.G., Davis, R.E., Feddema, J.J., Klink, K.M., Legates, D.R., Odonnell, J., Rowe, C.M., 1985. STATISTICS FOR THE EVALUATION AND COMPARISON OF MODELS. Journal of Geophysical Research-Oceans 90(NC5) 8995-9005.